Article

pubs.acs.org/Biomac

Effective Gene Delivery Using Stimulus-Responsive Catiomer Designed with Redox-Sensitive Disulfide and Acid-Labile Imine Linkers

Xiaojun Cai,[†,#] Chunyan Dong,[‡,#] Haiqing Dong,[†] Gangmin Wang,[†] Giovanni M. Pauletti,[∥] Xiaojing Pan,[§] Huiyun Wen,[†] Isaac Mehl,[†] Yongyong Li,*[,†] and Donglu Shi*[,†,⊥]

[†]The Institute for Advanced Materials and Nano Biomedicine, School of Medicine, [‡]Department of Oncology, Shanghai East Hospital, and [§]School of Life Science and Technology, Tongji University, Shanghai 200092, China

[∥]James L. Winkle College of Pharmacy and [⊥]School of Electronic and Computing Systems, College of Engineering and Applied Science, University of Cincinnati, Cincinnati, Ohio, 10 45221, United States

ABSTRACT: A dual stimulus-responsive mPEG-SS-PLL$_{15}$-glutaraldehyde star (mPEG-SS-PLL$_{15}$-star) catiomer is developed and biologically evaluated. The catiomer system combines redox-sensitive removal of an external PEG shell with acid-induced escape from the endosomal compartment. The design rationale for PEG shell removal is to augment intracellular uptake of mPEG-SS-PLL$_{15}$-star/DNA complexes in the presence of tumor-relevant glutathione (GSH) concentration, while the acid-induced dissociation is to accelerate the release of genetic payload following successful internalization into targeted cells. Size alterations of complexes in the presence of 10 mM GSH suggest stimulus-induced shedding of external PEG layers under redox conditions that intracellularly present in the tumor microenvironment. Dynamic laser light scattering experiments under endosomal pH conditions show rapid destabilization of mPEG-SS-PLL$_{15}$-star/DNA complexes that is followed by facilitating efficient release of encapsulated DNA, as demonstrated by agarose gel electrophoresis. Biological efficacy assessment using pEGFP-C1 plasmid DNA encoding green fluorescence protein and pGL-3 plasmid DNA encoding luciferase as reporter genes indicate comparable transfection efficiency of 293T cells of the catiomer with a conventional polyethyleneimine (bPEI-25k)-based gene delivery system. These experimental results show that mPEG-SS-PLL$_{15}$-star represents a promising design for future nonviral gene delivery applications with high DNA binding ability, low cytotoxicity, and high transfection efficiency.

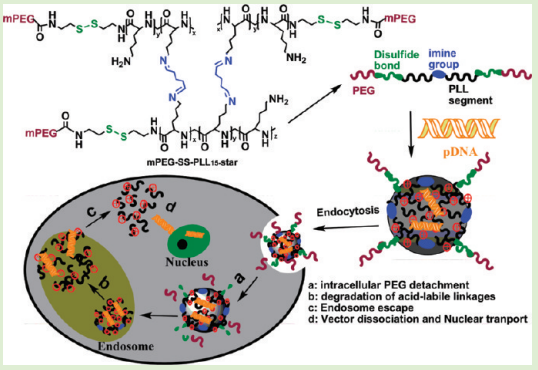

1. INTRODUCTION

Gene therapy is considered to be one of the most promising approaches to treat diseases of genetic defects. In gene therapy, genetic materials, either RNA or DNA, are transferred into specific human tissues or cells to replace defective genes, substitute missing genes, silence unwanted gene expression, or introduce new cellular biofunctions.[1] Clinical success of these interventions, however, relies on the development of efficient, nontoxic gene delivery vectors that are capable of mediating high and sustained levels of gene expression. Polyplexes formed by electrostatic interaction between cationic polymers (i.e., catiomers) and plasmid DNA (pDNA) have gained much attention as nonviral gene delivery vectors due to their respectable DNA loading capacity, easy of fabrication, limited immunogenicity, and versatility for chemical modifications.[2−5] Therapeutic efficacy of polyplex-mediated gene delivery strategies critically depends on effective condensation of genetic materials, successful distribution to desired target cells, cellular internalization, endosomal escape, efficient unpacking, and nuclear transport of genetic payload.[6,7] Throughout this journey, the chemical stability of encapsulated genetic materials must be guaranteed until it reaches the nucleus.[8] Inefficient escape from the endosomal compartment usually results in chemical degradation of DNA following cellular internalization of polyplexes.[9] Similarly, premature and incomplete unpacking of DNA from polyplexes significantly decreases transfection efficiency.[4,10] In addition, it has been recognized that cationic polyplexes are rapidly cleared from the circulatory system following interaction with negatively charged blood components.[11,12] Hence, innovative approaches that address these critical issues of nonviral gene delivery vectors are required to offer viable therapeutic options in the future.

Surface functionalization of catiomers using hydrophilic polymers such as poly(ethylene glycol) (PEG) has become a viable strategy to reduce positive surface charge of polyplexes and, consequently, the toxic side effects. In addition, surface

Received: December 6, 2011
Revised: March 2, 2012
Published: March 9, 2012

Scheme 1. Schematic Diagram Illustrating mPEG-SS-PLL$_{15}$-star Catiomer for pDNA Encapsulation and the Intracellular Stimulus-Responsive pDNA release

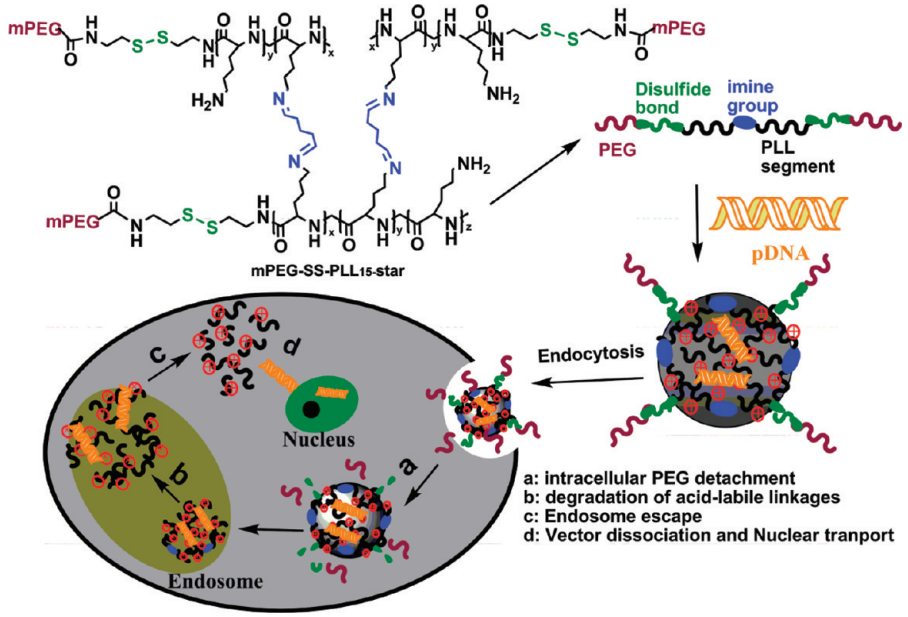

coverage with a PEG shell protects catiomer/DNA complexes from uptake by the reticuloendothelial system (RES), effectively prolonging in vivo circulation time.[13−16] Nevertheless, PEG-shielding has been demonstrated to reduce DNA binding,[17] cellular uptake,[18,19] and endosomal escape.[20−22] To solve this dilemma, previous research introduced catiomers bearing chemically cleavable PEG shells.[23,24] This design helps maintain the stability of the catiomer/DNA complex during biodistribution, at the desired target cell; however, removal or "shedding" of this hydrophilic surface layer enhances cellular interactions, thereby facilitating efficient internalization.[15] Various experiments demonstrated that transfection efficiency of lipid or polymer-based gene delivery systems fabricated with a cleavable PEG layer is superior to that of conventional polyplexes.[25−27] In particular, PEG shedding in response to a redox-sensitive stimulus has gained much interest for drug and gene delivery in cancer therapy, as the tumor microenvironment generally presents a higher concentration of the physiological reducing agent glutathione (GSH).[28,29] For example, Takae and coworkers reported a three-fold increase in gene transfection efficiency using PEG-detachable PEG-SS-P[Asp(DET)] micelles as nonviral delivery vector.[30] Similar results were recently reported from our studies where transfection efficiency in HeLa cells increased about three- to six-fold when mPEG-SS-PLL$_{45}$ polyplexes were used instead of mPEG-PLL$_{40}$ delivery vectors.[31]

Because the therapeutic payload of gene delivery vectors must be delivered into the nucleus, successful endosomal escape of the catiomer/DNA complex following cell internalization presents a critical step in gene therapy. This behavior was reported to be associated with the proton sponge effect of catiomer.[7] Protonation of catiomer induces rapid flux of ions and water into the subcellular compartment, eventually resulting in rupture of the endosomal membrane, followed by release of the entrapped compartments into the cytosol.[9] The high density of ionizable functional groups in polyethyleneimine (PEI) has been demonstrated to accelerate effectively endosomal escape.[32,33] In contrast, transfection efficiency of poly-L-lysine (PLL)-based gene delivery vectors is generally unsatisfactory because of its lower amine group density,[33] and most of the amine group has already been protonated at pH 7.4. To increase biologically efficacy, PLL has been chemically modified using various moieties that improve endosomal escape.[34] For example, incorporation of membrane-fusion peptide PAsp(DET) induces remarkable destabilization of the endosomal membrane structure during acidification.[35,36] Similarly, histidine-modified PLL also efficiently augments gene transfer.[37,38] Alternate chemical designs based on inclusion of acid-labile linkers such as acetal-ketal,[39] hydrazone,[15] orthoester,[5,40] and imine moieties[32] could also increase the transfection efficiency by accelerating the degradation of carriers in the acidic endosomal compartment and facilitate the release of payload pDNA.

On the basis of these findings, we engineered and developed a unique mPEG-SS-PLL$_{15}$-star catiomer that can combine redox-sensitive removal of an external PEG shell with acid-induced escape from the endosomal compartment. In particular, the rational design offers this catiomer with star polymer's distinct properties including a 3-D globular compact architecture that has unique properties compared with its linear analogs.[41−43] It is hypothesized that cleavage of the PEG layers in response to a reductive environment of intracellular or tumor microenvironment can effectively increase cellular uptake, as illustrated in Scheme 1. Subsequently, the acid-labile PLL segments cross-linked by imine linkers are expected to degrade in the acidic endosome, forming low-molecular-weight fragments such as mPEG-SS-PLL$_{15}$ that facilitates endosomal escape of therapeutically active DNA payload. The physicochemical properties of mPEG-SS-PLL$_{15}$-star were characterized to show the structural consequences of the polymer system upon exposure to high GSH concentrations and endosomal pH conditions. Gene transfection efficiency was evaluated in vitro using the pEGFP and pGL-3 pDNA as the reporter genes.

dx.doi.org/10.1021/bm2017355 | *Biomacromolecules* 2012, 13, 1024−1034

2. EXPERIMENTAL SECTION

2.1. Materials. Poly(ethylene glycol) monomethyl ether (mPEG, MW = 2000 g/mol) was purchased from Yare Biotech, and ε-benzyloxycarbonyl-L-lysine was purchased from GL Biochem. Succinic anhydride, glutaraldehyde (50% in water), cysteamine hydrochloride (98%), and triphosgene (99%) were purchased from Aladdin and used as received. Triethylamine (Et_3N, 99%, Sigma) was used as received. Tetrahydrofuran (THF), dichloromethane (DCM), and *N*,*N*-dimethyl formamide (DMF) were dried by refluxing over CaH_2, distilled, or vacuum-distilled before use. Hydrogen bromide (HBr) 33% (w/w) solution in glacial acetic acid was purchased from ACROS Organics. Dulbecco's modified Eagle's medium (DMEM), Dulbecco's phosphate buffered saline (PBS), 3-(4,5-dimethyl-thiazol-2-yl)-2,5-diphenyltetrazolium bromide (MTT), trypsin-EDTA, fetal bovine serum (FBS), and penicillin-streptomycin were purchased from Gibco Invitrogen. Dialysis bags (Spectra/Por 7) were purchased from Spectrum Laboratories. Branched poly(ethylenimine) (bPEI-25 k, MW = 25 000 g/mol) was obtained from Aldrich-Sigma Chemical. Block copolymer mPEG-PLL_{40} without disulfide bonds was synthesized by our laboratory. Label IT Tracker intracellular nucleic acid localization kit Cy3 was purchased from Mirus Bio. BCA protein assay kit was purchased from Pierce. Luciferase assay system and reporter lysis buffer were purchased from Promega. The reporter plasmids, pEGFP-C1 and pGL-3, were purchased from Invitrogen and stored at −20 °C until transfection experiments.

2.2. Synthesis of mPEG-SS-$PzLL_{15}$ Intermediate. The synthesis of mPEG-SS-$PzLL_{15}$ was accomplished according to the following strategy: (i) preparation of zLL-NCA; (ii) preparation of mPEG-SS-NH_2; and (iii) ring-opening polymerization of zLL-NCA initiated by mPEG-SS-NH_2.

ε-Benzyloxycarbonyl-L-lysine (zLL, 5.6 g, 20 mmol) was suspended in dry THF (50 mL) at 50 °C, and triphosgene (2.5 g, 8.4 mmol) was slowly added under nitrogen. Following completion of the reaction, crude zLL-NCA was precipitated with excess dry *n*-hexane and further purified by crystallizing using THF/*n*-hexane (1:15, v/v).

The mPEG-SS-NH_2 intermediate was prepared following a protocol previously published by our laboratory.[31] In brief, *N*-hydroxysuccinimide (NHS) (0.07 g, 0.6 mmol), *N*,*N*′-dicyclohexylcarbodiimide (DCC) (0.12 g, 0.6 mmol), and mPEG-COOH (1.0 g, 0.5 mmol) were dissolved in DCM (30 mL) at 0 °C for 5 h. Subsequently, a dry solution of cysteamine (0.5 g, 3.5 mmol) in 5 mL of DCM was added dropwise, and the reaction was maintained at room temperature (RT) for additional 24 h under a dry nitrogen atmosphere. The product was isolated by filtration to remove insoluble byproducts, precipitated twice in cold diethylether and purified by 24 h of dialysis (MW cutoff: 1000 Da) against water. mPEG-SS-NH_2 was collected after lyophilization (NMR (ppm): 3.55 (−C**H**$_2$C**H**$_2$O−), 3.4 (−C**H**$_3$O), 2.5 (−SS−C**H**$_2$−C**H**$_2$−NH−), 2.35 (−SS−C**H**$_2$−CH$_2$−NH−)).

mPEG-SS-NH_2 and zLL-NCA were combined in dry DMF at a molar ratio of 1:15. Ring-opening polymerization was allowed to proceed for 3 days at RT. The desired mPEG-SS-$PzLL_{15}$ was purified by 24 h of dialysis (MW cutoff: 3500 Da) against water and collected after lyophilization.

2.3. Synthesis of Redox-Sensitive mPEG-SS-PLL_{15} Catiomer. mPEG-SS-$PzLL_{15}$ was dissolved in 10 mL of trifluoroacetic acid (TFA) and combined with two mole equivalents (with respect to the benzyl carbamate group) of a 33% (w/w) HBr solution in acetic acid. The solution was stirred at 0 °C for 1 h under nitrogen and precipitated in excess diethyl ether. The crude product was dissolved in DMF and dialyzed (MW cutoff: 3500 Da) for 6 h against distilled water containing a few drops of ammonia solution (pH 9.0) to remove the HBr. After refreshing with pure distilled water, the crude product was dialyzed for an additional 48 h. Deprotected mPEG-SS-PLL_{15} was collected after lyophilization.

2.4. Synthesis of Dual Stimulus-Responsive mPEG-SS-PLL_{15}-star Catiomer. mPEG-SS-PLL_{15} was dissolved in double-distilled water using a 50 mL two-necked flask, and an aqueous solution of glutaraldehyde was added dropwise over 2 h under vigorous stirring at RT. The reaction mixture was stirred for additional 4 h before dialysis (MW cutoff: 3500 Da) for 24 h against water. The purified dual stimulus-responsive mPEG-SS-PLL_{15}-star catiomer was collected after lyophilization.

2.5. Chemical Properties of mPEG-SS-PLL_{15}-star Catiomer. Proton nuclear magnetic resonance (^{1}H NMR) spectra were recorded on the Advance500 MHz spectrometer (Switzerland) using DMSO-d_6 as solvent and TMS as standard. Molecular weight analysis was performed using the Applied Biosystems 4700 Proteomics (TOF/TOF) Analyzer (Framingham, MA). The UV Nd:YAG laser was operated at a 200 Hz repetition rate wavelength of λ = 355 nm. Accelerated voltage was operated at 20 kV under batch mode acquisition control. The solution was 0.001:1:2 (v/v) TFA/acetonitrile (ACN)/water. Mass spectral data were processed using Data Explorer 4.0 (Applied Biosystems).

2.6. Cell Viability Assay. Human embryonic kidney transformed 293 (293T) and human cervix carcinoma (HeLa) cells were obtained from the Cell Center of the Tumor Hospital at Fudan University and routinely maintained at 37 °C in a humidified 5% (v/v) CO_2 atmosphere using DMEM supplemented with 10% FBS and 0.1% (v/v) penicillin/streptomycin solution. Cell viability in the presence and absence of various mPEG-SS-PLL_{15}-star catiomers was determined using the MTT assay. mPEG-SS-PLL_{15} and bPEI-25k served as control. In brief, 293T and HeLa cells were seeded into a 96-well plate at a density of 5×10^3 cells/well. Following an overnight attachment period, cells were exposed to various catiomer concentrations (13.2 to 225 mg/L) prepared in cell culture medium. After 24 h, the medium was replaced with 200 μL of fresh DMEM, 20 μL of a MTT solution (5 mg/mL) in PBS pH 7.4 was added, and the plate incubated at 37 °C for additional 4 h. Subsequently, the culture medium was removed and 150 μL of DMSO was added to each well, and after an additional 10 min of incubation at 37 °C optical density (OD) was measured at λ = 492 nm using the Multiscan MK3 plate reader (Thermo Fisher Scientific, Waltham, MA). The relative cell viability in percent (%) was calculated according to: (OD sample/OD control) × 100%, where OD control was measured in the absence of the polymers and OD sample in the presence of the polymers. Each concentration was studied using six independent experiments.

2.7. Buffering Capacity of mPEG-SS-PLL_{15}-star Catiomers. Relative buffering capacities of mPEG-SS-PLL_{15}-star catiomers and bPEI-25k were compared using acid−base titration. Polymers were dissolved at 200 mg/L in 50 mM NaCl solution. Initially, the pH value of this solution was adjusted to pH 10 using 0.1 M NaOH. Sequentially, 0.1 M HCl aliquots were added and pH value was measured after each addition using a microprocessor pH meter.

2.8. Fabrication of mPEG-SS-PLL_{15}-star/pDNA Complexes. A pDNA stock solution (120 ng/μL) was prepared in 40 mM Tris-HCl buffer (pH 7.4). Separately, mPEG-SS-PLL_{15}-star was dissolved in 150 mM NaCl at 2 mg/mL, and the solution was cleared by filtration (0.22 μm). Polyplexes were formed by adding mPEG-SS-PLL_{15}-star with a desired concentration to pDNA stock solution, resulting in catiomer/pDNA ratios ranging from 0:1 to 8:1 w/w for agarose gel retardation assay and 1:1 to 10:1 w/w for particle size distribution and zeta potential measurement. Complexes were vortexed gently, then allowed to incubate for 30 min at 37 °C before use.

2.9. Agarose Gel Retardation Assay. To assess the ability of catiomers to condensate DNA into electrostatically stabilized polyplexes, we performed the agarose gel retardation assay. Routinely, catiomer/pDNA complex suspensions containing 0.1 μg of pDNA were loaded onto 1% (w/v) agarose gel containing ethidium bromide. Electrophoretic separation was carried out for 40 min at 120 V in Tris-acetate running buffer. DNA bands were visualized at λ = 254 nm using an Imago GelDoc system.

2.10. Particle Size Distribution and Zeta Potential. To determine relevant physicochemical properties of polyplexes, we measured particle size distribution and zeta potential of fabricated catiomer/pDNA complexes containing 1 μg pDNA by Nano-ZS 90 Nanosizer (Malvern Instruments, Worcestershire, U.K.) according to the manufacturer's instructions. If required, polyplex suspension was diluted with 150 mM NaCl.

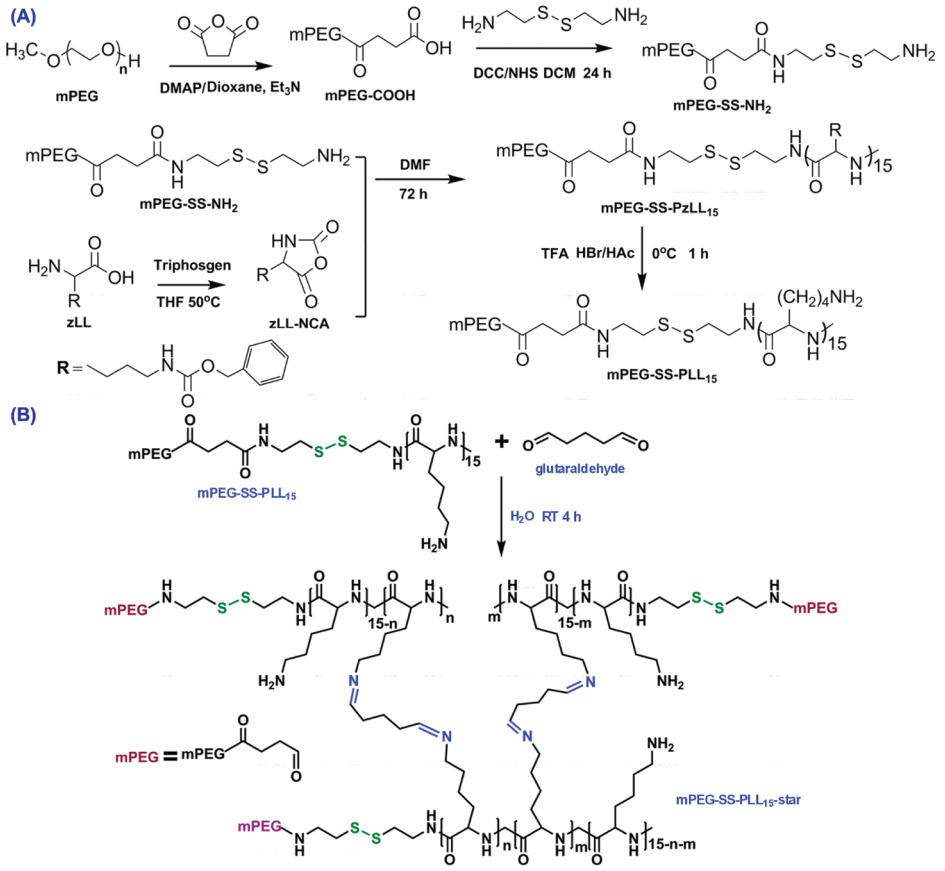

Figure 1. Synthesis of novel mPEG-SS-PLL_{15} cationers (A) and reaction scheme for copolymerization of mPEG-SS-PLL_{15} in the presence of glutaraldehyde (B).

2.11. Transmission Electronic Microscopy (TEM). To visualize mPEG-SS-PLL_{15}-star/pDNA association complexes, polyplexes were prepared at a weight ratio of 5:1 and observed in a Hitachi H-7100 transmission electron microscope using an acceleration voltage of 100 kV.

2.12. Stability of mPEG-SS-PLL_{15}-star/pDNA Complexes. The rational design of mPEG-SS-PLL_{15}-star predicts redox-induced cleavage of external PEG shell and acid-induced hydrolysis of the cross-linked polymer structure. Experimentally, the stability of mPEG-SS-PLL_{15}-star/pDNA complexes in response to 10 mM GSH was determined following a protocol previously published.[29] In brief, mPEG-SS-PLL_{15}-star/pDNA polyplexes were formed in 150 mM NaCl at a weight ratio of 5:1, and an adequate amount of GSH was added to establish a 10 mM GSH solution mimicking intracellular or tumor microenvironment redox conditions. Time-dependent changes in particle size distribution of this suspension were monitored by dynamic laser light scattering (DLS) for up to 4.5 h. Similarly, physical stability of fabricated polyplexes at a weight ratio of 5:1 was measured at pH 5.0, mimicking the environment of acidified endosomes. Following preparation of mPEG-SS-PLL_{15}-star/pDNA complexes at desired weight ratios, an adequate volume of HCl was added to adjust the solution pH to 5.0. Subsequently, particle size distribution was monitored for 2.5 h by DLS, as described above. For determination of the implications of physical changes in particle size distribution on genetic payload release from mPEG-SS-PLL_{15}-star/pDNA complexes in the presence of 10 mM GSH and pH 5.0, aliquots of the polyplex suspension conditions were removed and subjected to gel electrophoresis as described above.

2.13. In Vitro Transfection Efficiency of mPEG-SS-PLL_{15}-star Polyplexes. Biological activity of fabricated gene delivery vectors was assessed in vitro using pGL-3 and pEGFP pDNA as reporter gene, mPEG-PLL_{40} and PEI at its optimal ratio (w/w = 1.3:1) as the control.[44,45] Transfection experiments were performed with 293T cells in 24-well plates at a density of 5×10^4 cells/well. pGL-3-containing polyplexes fabricated at various w/w ratios ranging from 1:1 to 10:1 were suspended in serum-free DMEM and added to each well (1 μg DNA/well). Following a 4 h incubation at 37 °C in a humidified atmosphere with 5% (v/v) CO_2, the medium was replaced with fresh DMEM containing 10% FBS, and cells were incubated for additional 44 h to allow gene expression. For luciferase assay, the medium was removed, and the cells were washed with 0.25 mL of PBS, pH 7.4, then the cells were lysed using 200 μL of reporter lysis buffer (Promega, USA). The luciferase activity was measured with chemiluminometer (GloMax-Multi, Promega, USA) according to manufacture's protocol. Luciferase activity was normalized to the amount of total protein in the sample, which was determined using a BCA protein assay kit (Pierce).

For flow cytometry study, pEGFP-containing polyplexes (w/w 5:1 and 10:1) were separately transferred to 293T cells in terms of the aforementioned method. At 44 h post-transfection, pEGFP-expressing cells were first visualized under a Nikon Ti−S inverted microscope equipped with a fluorescence attachment. For flow cytometry assessment, cells were washed with PBS, pH 7.4, trypsinized, and collected in sterile tubes after a 5 min centrifugation at 1000 rpm. The supernatant was discarded, and cells were washed twice with PBS, pH 7.4 containing 2% (v/v) FBS and 2 mM EDTA, respectively. Cells were fixed in the dark at 4 °C for 5 min using a 2% (w/v) paraformaldehyde solution prepared in PBS, pH 7.4. Quantitative analysis of viable pEGFP-expressing cells was performed by flow cytometry (FACScan, Becton & Dickinson). The instrument was calibrated with nontransfected cells (negative control) to identify viable cells, and the percent of pEGFP-positive cells was determined from fluorescence scan performed with ~1×10^4 cells using the FL1-H channel.

2.14. Observation of the Intracellular DNA Transport. The ability of fabricated gene delivery vectors to transport pEGFP to the cytoplasm and nucleus was evaluated using confocal laser scanning

dx.doi.org/10.1021/bm2017355 | Biomacromolecules 2012, 13, 1024−1034

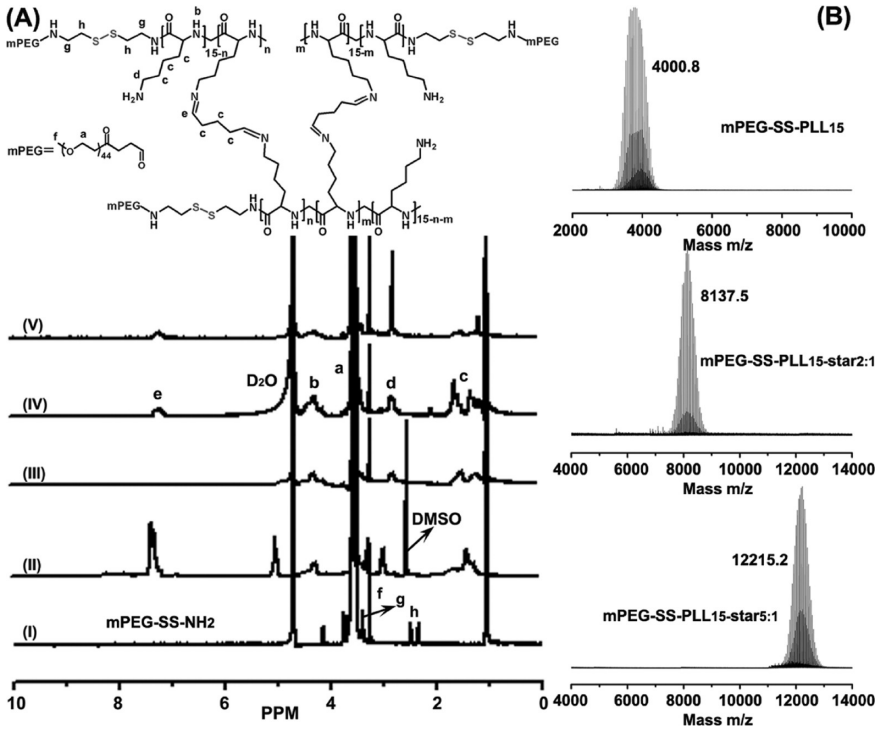

Figure 2. Spectroscopic analysis of fabricated catiomers. Representative ^{1}H NMR spectra of mPEG-SS-NH_2 (I), mPEG-SS-PzLL$_{15}$ (II), mPEG-SS-PLL$_{15}$ (III), mPEG-SS-PLL$_{15}$-star$_{2:1}$ (IV), and mPEG-SS-PLL$_{15}$-star$_{5:1}$ (V) are summarized in panel A. The mass spectrum of mPEG-SS-PLL$_{15}$, mPEG-SS-PLL$_{15}$-star$_{2:1}$, and mPEG-SS-PLL$_{15}$-star$_{5:1}$ batch is shown in panel B.

microscope. 293T cells were seeded in six-well plates at a density of 1 × 10^5 cells/well. Five μg pEGFP was intercalated with 5 μL of 10 mM Cy3 for 60 min at 37 °C before the addition of catiomer.[33,46] Subsequently, labeled pEGFP was purified by precipitating twice in cold ethanol 100% and rinsing in ethanol 70%, then resuspended in 10 μL of sterile water. The Cy3-labeled pEGFP-containing complexes at optimal catiomer/pDNA ratios were prepared and added to each well. Following 4 h of incubation at 37 °C, complexes were removed and cells were washed with PBS for three times, fixed with 4% paraformaldehyde, and washed with PBS twice, respectively. The cell nuclei was stained with 0.5 mL of DAPI (100 ng/mL) for 10 min at 37 °C, after which the cells were further washed with PBS three times. The fluorescence of Cy3-labeled pEGFP was visualized and recorded by Leica TCS SP5 II fluorescence microscopy with a 63×oil immersion objective.

3. RESULTS AND DISCUSSION

3.1. Synthesis of Dual Stimulus-Responsive mPEG-SS-PLL$_{15}$-star Catiomer. The dual stimulus-responsive star catiomer mPEG-SS-PLL$_{15}$-star was designed with a redox-sensitive disulfide bond between the PEG and PLL moieties in addition to acid-labile imine linkers between individual PLL units. The design rationale is based on the desire to remove the external PEG shell in the presence of tumor-relevant GSH concentrations, thus augmenting intracellular uptake. Following successful internalization into target cells, acid-catalyzed hydrolysis of the imine moieties in the endosome is anticipated to accelerate the release of the genetic payload from this subcellular compartment, which is a necessary prerequisite for gene transfer into the nucleus. The synthesis of this multifaceted catiomer is illustrated in Figure 1. In brief, mPEG-SS-PzLL$_{15}$ was prepared by ring-opening polymerization of zLL-NCA using mPEG-SS-NH_2 as initiator. After deprotection, mPEG-SS-PLL$_{15}$ was reacted with glutaraldehyde affording the desired catiomer mPEG-SS-PLL$_{15}$-star that contains redox-sensitive disulfide bonds and acid-labile imine linkers. The ^{1}H NMR spectra of selected mPEG-SS-PLL$_{15}$-star catiomers and relevant precursors are shown in Figure 2. In addition to distinct resonance peaks for the PEG and PLL blocks, the presence of a peak around 7.15 ppm, which is attributed to protons of the imine group (−C═NH−), indicated the successful synthesis of the acid-labile mPEG-SS-PLL$_{15}$-star catiomer. This conclusion is supported by mass spectrometry data that reveal a significant increase in the average molecular weight of the cross-linked catiomers mPEG-SS-PLL$_{15}$-star$_{5:1}$ and mPEG-SS-PLL$_{15}$-star$_{2:1}$, respectively (Table 1). For comparison, the mean molecular weight of the mPEG-SS-PLL$_{15}$ intermediate was determined as 4000 g/mol. The number of zLL residues per PEG chain was estimated by relative integration of the ^{1}H signals corresponding to the methylene group at δ 3.55 and the phenyl ring at δ 7.32 in mPEG-SS-PzLL spectrum. These results suggest a 1:15 ratio between mPEG-SS-NH_2 and zLL-NCA moieties. Hence, the redox-sensitive catiomer was designated as mPEG-SS-PLL$_{15}$.

Table 1. Physicochemical Properties of Crosslinked mPEG-SS-PLL$_{15}$ Catiomers

	initial concentration (mol/L)		initial molar ratio			
no.	mPEG-SS-PLL$_{15}$	dialdehyde	mPEG-SS-PLL$_{15}$	dialdehyde	solubility in water	M_w
1	0.005	0.025	1	5	no	n.a.
2	0.004	0.004	1	1	no	n.a.
3	0.004	0.002	2	1	yes	8137
4	0.00125	0.00025	5	1	yes	12 215

Using this redox-sensitive precursor, the acid-labile mPEG-SS-PLL$_{15}$-star catiomer was obtained by reacting the amino

dx.doi.org/10.1021/bm2017355 | Biomacromolecules 2012, 13, 1024−1034

group in the Lys side chains with glutaraldehyde via a Schiff base reaction. Copolymerization was controlled by defined molar ratios of starting materials, their respective concentration in the reaction mixture, the rate of addition, and the reaction temperature. Physicochemical properties of cross-linked catiomers are summarized in Table 1. The results underline that successful preparation of water-soluble copolymers is only feasible in diluted solutions using molar mPEG-SS-PLL$_{15}$/glutaraldehyde ratios >1. These findings are consistent with previous studies performed with cross-linked PEI copolymers.[32]

3.2. DNA Complexation with mPEG-SS-PLL$_{15}$-star Catiomers. Electrostatic interactions between negatively charged DNA and positively charged polymers facilitate the formation of partially or completely neutralized association complexes (i.e., polyplexes). As a consequence, successful condensation of DNA with catiomers results in retardation or complete loss of oriented DNA migration within an electric field. We compared the ability of fabricated catiomers to complex pDNA at weight ratios ranging from 1:1 to 8:1 using agarose gel electrophoresis (Figure 3). The results revealed that

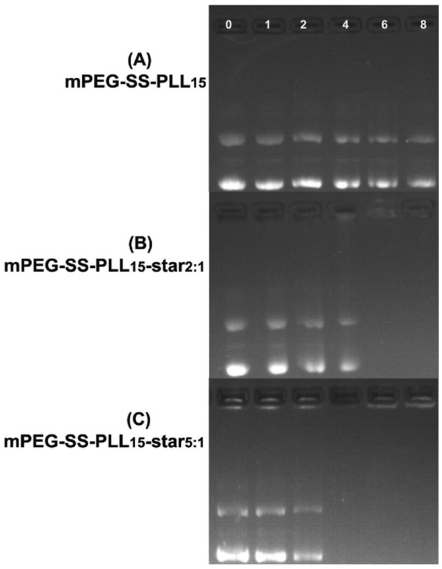

Figure 3. DNA complexation with mPEG-SS-PLL$_{15}$-based catiomers. Agarose gel electrophoresis was performed as outlined in the Experimental Section using mixtures of mPEG-SS-PLL$_{15}$ (A), mPEG-SS-PLL$_{15}$-star$_{2:1}$ (B), and mPEG-SS-PLL$_{15}$-star$_{5:1}$ (C) with pDNA prepared at weight ratios ranging from 0:1 to 8:1. Representative gels were visualized at λ = 254 nm.

mPEG-SS-PLL$_{15}$ does not effectively condensate pDNA at a weight ratio up to 8:1 (Figure 3A). Consistent with previous findings by us,[31] it is hypothesized that the low amino group density in mPEG-SS-PLL$_{15}$ impedes effective formation of electrostatically stabilized pDNA/catiomer association complexes. However, following cross-linking with glutaraldehyde, the ability of the fabricated polymers to condensate pDNA remarkably increases. For mPEG-SS-PLL$_{15}$-star$_{2:1}$, the absence of a UV-intensive band at weight ratios >4:1 implies effective pDNA condensation (Figure 3B). It is hypothesized that the cross-linked polymer harbors a significantly increased number of cationic PLL moieties, which effectively augments pDNA binding capacity of the catiomer. Experimentally, this was confirmed by demonstrating that mPEG-SS-PLL$_{15}$-star$_{5:1}$, which was fabricated using an initial molar mPEG-SS-PLL$_{15}$/glutaraldehyde ratio of 5:1, shows superior pDNA binding capacity when compared with mPEG-SS-PLL-star$_{2:1}$ (Figure 3C).

3.3. Buffering Capacity. Optimal gene transfection requires transfer of the genetic payload into the nucleus. Following cellular internalization, escape from endosomal vesicles represents the major limitation for gene delivery systems.[47] The proton sponge effect of a synthetic gene delivery vector has been reported to be a key factor in swelling of endocytic vesicles, escaping into the cytosol and overall gene transfection efficiency.[48,49] The catiomers fabricated in this study contain PLL blocks that may act as a proton sponges. In addition, the presence of acid-labile imine linkers in these polymers is expected to enhance endosomal escape by rapidly breaking down these high-molecule-weight catiomers into low-molecule-weight counterparts under endosome or lysosome low-pH conditions (pH 5.5). A significant buffering capacity associated with a catiomer positively increases endosomal escape as a consequence of remarkable acidification within this subcellular compartment.[47] We, therefore, quantified the buffering capacity of different polymeric solutions following serial addition of HCl aliquots. The results from these titration experiments are summarized in Figure 4. A 200 mg/L solution

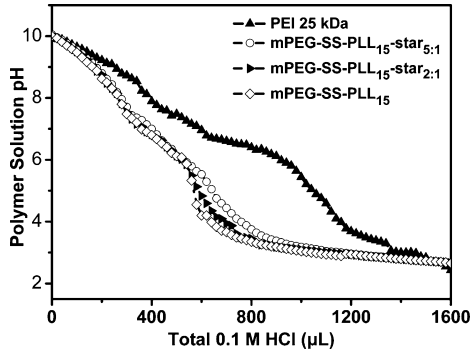

Figure 4. Buffering capacity of catiomers. Polymer solutions (200 mg/L) were adjusted to pH 10 using 0.1 M NaOH. Subsequently, aliquots of 0.1 M HCl were added, and solution pH was recorded. Representative plots are shown for different mPEG-SS-PLL$_{15}$-star catiomers and bPEI-25k.

of bPEI-25k displayed a remarkable buffering capacity attributed to its multiamine structure that contains a mixture of primary, secondary, and tertiary amines groups. In contrast, the buffering capacity of mPEG-SS-PLL catiomers was significantly lower. mPEG-SS-PLL$_{15}$ displayed the lowest buffering capacity among all catiomers studied, which may result from its uniform composition of primary amines only. After being cross-linked with glutaraldehyde, a slight increase in buffering capacity of mPEG-SS-PLL$_{15}$-star catiomers was observed, which is possibly due to the generation of more fractions of secondary amines.

3.4. Cellular Viability Assessment. Clinical success of synthetic gene delivery vectors critically depends on meeting an acceptable safety profile in addition to therapeutic efficacy. In this study, in vitro cytotoxicity of fabricated catiomers was evaluated using the 293T and HeLa cell lines. In the presence of bPEI-25k (positive control), cell viability rapidly decreased to a limiting value around 20% at concentrations >25 mg/L (Figure 5). Previous studies demonstrated that the cationic charge density of PEI is responsible for this dramatic reduction in cell viability.[50] In contrast, mPEG-SS-PLL$_{15}$-based polymers

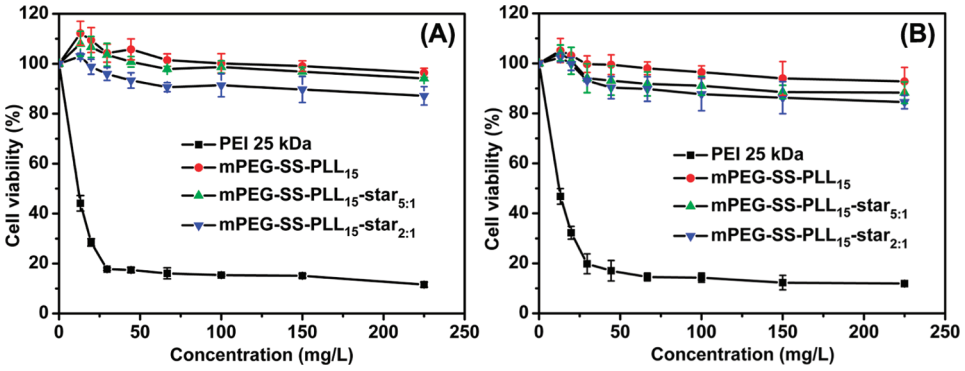

Figure 5. Dose-dependent cytotoxicity of mPEG-SS-PLL_{15}-star catiomers. Viability of 293T (A) and HeLa (B) cells following a 24 h incubation with various concentrations of PEI (positive control) or mPEG-SS-PLL_{15}-based polymers was quantified using the MTT assay. Data are shown as mean ± SD (n = 6).

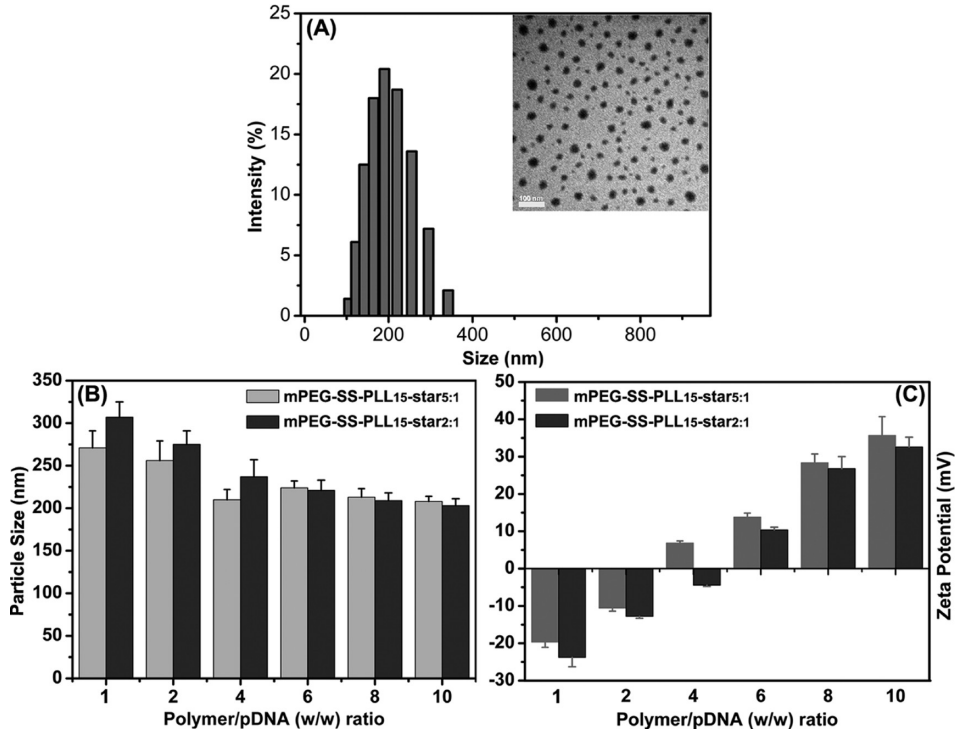

Figure 6. Size distribution of mPEG-SS-PLL_{15}-$star_{5:1}$/pDNA complex. Polyplexes were prepared in 150 mM NaCl at a weight ratio of 5:1. Results from DLS and TEM (inset) of a representative polyplex batch are shown (A). Impact of catiomer/pDNA ratio on physicochemical polyplexes characteristics. Mean particle size (B) and zeta potential (C) were determined for mPEG-SS-PLL_{15}-star/pDNA polyplexes fabricated in 150 mM NaCl at various weight ratios. Data are shown as mean ± SD (n = 3).

exhibited a remarkably increased cellular viability profile even at concentrations of 225 mg/L. Throughout the entire concentration range tested, cell viability was always maintained >90% following a 4 h incubation (Figure 5). Previous data demonstrated that mPEG-SS-PLL_{15}-$star_{5:1}$ is capable of effective DNA condensation, implying high positive charge density (Figure 3). Nevertheless, the cellular viability of mPEG-SS-PLL_{15}-$star_{5:1}$ is superior to conventional PEI. We predict that the presence of acid-labile imine linkers facilitates rapid degradation of the catiomer into less toxic, low-molecular-weight fragments under acidic conditions present in the endosome. As a consequence, cytotoxicity of fabricated mPEG-SS-PLL_{15}-star polymer is dramatically reduced, suggesting favorable clinical utility for gene delivery applications.

3.5. Complexes of pDNA with mPEG-SS-PLL_{15}-star Catiomers. Particle size distribution, morphology, and surface charge of catiomer/pDNA polyplexes strongly influence cytotoxicity, cellular uptake/intracellular trafficking, and release of genetic payload.[46] Morphometric analysis of mPEG-SS-PLL_{15}-$star_{5:1}$/pDNA complexes was performed by DLS and TEM, respectively. The particle size distribution shown in Figure 6A reveals near-Gaussian distribution of polyplexes between 100 and 350 nm, with a mean diameter of ~200 nm. The inset in Figure 6A shows a representative TEM image where polyplexes are visible as spherical aggregates with diameters between 20 and 50 nm. The apparent discrepancy in size characteristics between the two methods is predicted to arise from evaporation of water required during TEM sample preparation.

The impact of different polymer/pDNA weight ratios on mean particle size and zeta potential of polyplexes is summarized in Figure 6B,C. These data show a reduction in

dx.doi.org/10.1021/bm2017355 | Biomacromolecules 2012, 13, 1024−1034

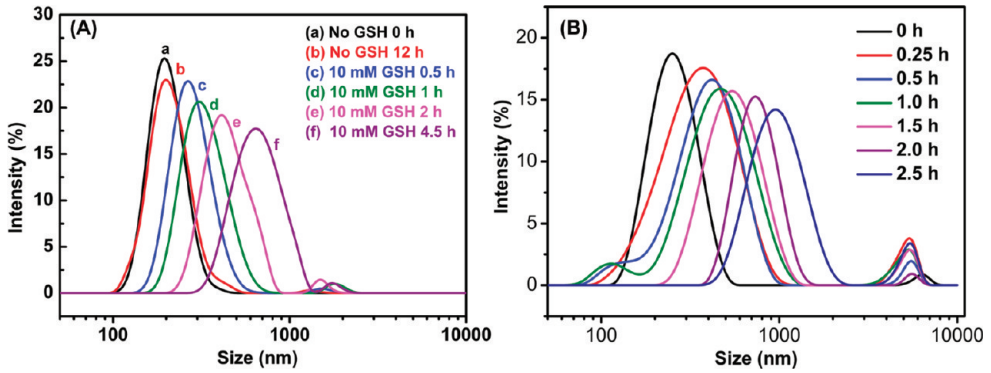

Figure 7. Time-dependent changes in size distribution of mPEG-SS-PLL$_{15}$-star$_{5:1}$/pDNA complexes as determined by DLS in the presence and absence of 10 mM GSH (A) and endosome-relevant pH conditions of pH 5.0 (B). Results are shown for one representative polyplex batch.

particle size with increasing catiomer concentration combined with the phenomenon of the disappearance of aggregates of naked DNA with a diameter around 800 nm (data not shown), implying very effective DNA condensation in the presence of increasing cationic polymer. At a weight ratio >4:1, the particle size of catiomer/pDNA complexes was ∼220 nm, which is believed to be within the optimum size range associated with efficient cellular uptake.[51] In parallel, the zeta potential of these complexes significantly increases from −20 to +30 mV when catiomer/pDNA weight ratio was increased from 1:1 to 10:1. The dramatic shift in zeta potential indicates neutralization of negative charge of polymer-associated pDNA at a weight ratio of 4:1. These results are consistent with previous electrophoretic mobility data shown in Figure 3. Further increase in catiomer content is hypothesized to lead to an excess of positively charged amine groups of the surface of these polyplexes. Eventually, charge−charge repulsion limits particle formation to a mean diameter around 200 nm and zeta potential of +30 mV. In general, the appropriate particle size and zeta potential of catiomer/pDNA complexes can facilitate the effective internalization into desired targeted cells.

3.6. Bioresponsive Properties of mPEG-SS-PLL$_{15}$-star$_{5:1}$/pDNA Complexes. Stimulus-responsive polymeric nanocarriers have attracted increasing interest for gene delivery applications in recent years because they can greatly enhance intracellular release of genetic payload and usually exhibit lower cytotoxicity.[52,53] In this study, we introduce a novel, dual-responsive catiomer design that contains redox-sensitive disulfide bonds and acid-labile imine linkers. To explore the consequences of these engineered labile linkers under simulated, cell-relevant conditions, we measured size changes of mPEG-SS-PLL$_{15}$-star$_{5:1}$/pDNA complexes in the presence and absence of 10 mM GSH, pH 7.4 (i.e., intracellular redox environment) and pH 5.0 (i.e., acidified endosomal compartment). Exposure of mPEG-SS-PLL$_{15}$-star$_{5:1}$/pDNA complexes for 12 h to PBS, pH 7.4 in the absence of GSH did not significantly alter the particle size distribution implying substantial stability of these polyplexes during biodistribution (Figure 7A). Inclusion of 10 mM GSH, however, rapidly increased the mean particle size, suggesting the formation of large aggregates (>650 nm) within hours. From these data, it is concluded that reductive cleavage of disulfide bonds engineered into this novel catiomer design removes the hydrophilic PEG layer on the exterior of the polyplexes. As a consequence, ionic interactions between positively and negatively charged centers of individual smaller particles result in the formation of larger aggregates. These results underline the feasibility of shedding the hydrophilic PEG layer after internalization into target cells, which is a necessary step in accelerating efficient gene transfer into the nucleus. Because the intracellular tumor environment generally contains increased GSH concentrations due to adaptive upregulation of antioxidant mechanisms in response to intrinsic oxidative stress,[54] redox-induced cleavage of the protective PEG shell may also augment tumor-selective delivery of therapeutic payload.

One major limitation of conventional gene delivery vectors is inadequate release from the endosomal compartment after successful internalization into desired target cells.[8] In the rational design of mPEG-SS-PLL$_{15}$-star catiomers, we engineered acid-labile imine linkers that are predicted to hydrolyze under endosome-relevant acidic pH conditions. The results shown in Figure 7B clearly demonstrate a rapid increase in the mean particle size following exposure of mPEG-SS-PLL$_{15}$-star$_{5:1}$/pDNA complexes to pH 5.0. We attribute the formation of larger aggregates (>1000 nm) to acid-induced hydrolysis of the imine moieties resulting in low-molecular-weight fragments, including mPEG-SS-PLL$_{15}$, that are unable to condense effectively DNA (Figure 3), thus resulting in the formation of much looser states of complexes with larger sizes. Combined, these results imply synergistic effects of redox-induced disulfide bond cleavage and pH-accelerated imine hydrolysis in rapidly destabilizing these gene delivery vectors that, ultimately, may translate into increased transfection efficiency.

3.7. Stimulus-Induced DNA Release from mPEG-SS-PLL$_{15}$-star Polyplexes. To investigate consequences of stimulus-induced size alterations of mPEG-SS-PLL$_{15}$-star/pDNA polyplexes on encapsulated payload, we used agarose gel electrophoresis to assess DNA migration properties in response to 10 mM GSH and pH 5.0, respectively. The results in Figure 8 demonstrate that DNA migration at pH 7.4 was completely inhibited using mPEG-SS-PLL$_{15}$-star/pDNA complexes at a weight ratio >2 (Figure 8A). Incubation for 30 min in the presence of 10 mM GSH, however, effectively allowed migration of negatively charged DNA toward the cathode from polyplexes fabricated at a catiomer/pDNA ratio ≤6 (Figure 8B). Combined with results from previous particle size measurements performed under identical conditions (Figure 7), we conclude that reductive cleavage of the PEG layer facilitates the release of DNA from these electrostatically stabilized association complexes. Furthermore, short-term exposure to pH 5.0 results in visible pDNA migration using polyplexes prepared with mPEG-SS-PLL$_{15}$-star at weight ratios ≤8 (Figure 8C). These data underline the possibility of synergistically utilizing redox-induced disulfide cleavage and

dx.doi.org/10.1021/bm2017355 | *Biomacromolecules* 2012, 13, 1024−1034

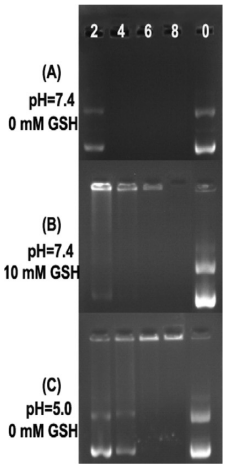

Figure 8. Stimulus-induced release of pDNA from mPEG-SS-PLL$_{15}$-star polyplexes. Association complexes were incubated for 30 min in PBS, pH 7.4 (A), PBS, pH 7.4 + 10 mM GSH (B), or PBS, pH 5.0 (C) before electrophoresis using a 1% agarose gel. Representative gel picture was show for each condition.

acid-catalyzed hydrolysis of imine linkers to control DNA release from polyplexes. In addition, it is found that pH-induced hydrolysis of the polymeric structure of mPEG-SS-PLL$_{15}$-star can accelerate payload release but only slightly more effective compared with reductive cleavage of the PEG shell. Nevertheless, stimulus-induced removal of the PEG layer triggered by increased GSH concentrations may lead to tumor-selective accumulation due to a persistent oxidative stress in the tumor microenvironment.[55] This is expected to augment cellular internalization of these gene delivery vectors, followed by acid-catalyzed degradation of high-molecular-weight PLL blocks, thus enhancing endosomal escape. As a consequence of this sequential, release mechanism, the overall transfection efficiency in tumor cells may be significantly enhanced.

3.8. Transfection Efficiency of mPEG-SS-PLL$_{15}$-star Polyplexes. To assess the biological efficacy of these novel gene delivery vectors, here we performed luciferase transfection assay, fluorescence microscopy, and flow cytometry with 293T cells and bPEI-25k as a positive control. Luciferase assay was carried out using different catiomer/pGL-3 weight ratios ranging from 1:1 to 10:1, and a weight ratio dependence of gene transfection efficacies is shown in Figure 9. All polyplexes exhibited the highest gene transfection efficiency at weight ratio of 6:1. It is intriguing that the highest efficiency for mPEG-SS-PLL$_{15}$-star$_{5:1}$ was 1.9×10^8 RLU/mg protein, approaching the same order of transgenetic efficacy as the well-known bPEI-25k (2.9×10^8 RLU protein at weight ratio of 1.3:1). Therefore, these novel, synthetic gene delivery vectors are capable of displaying extremely high transfection efficacies in an in vitro system.

pEGFP expression in 293T cells following exposure to mPEG-SS-PLL$_{15}$-star/pEGFP complexes fabricated at weight ratios of 5:1 and 10:1, respectively, was qualitatively evaluated by fluorescence microscopy and quantitatively assessed using flow cytometry. The high density of fluorescent cells visible under the microscope after transfection with both mPEG-SS-PLL$_{15}$-star-, mPEG-PLL$_{40}$-, and PEI-based polyplexes demonstrates successful delivery of pEGFP into the nucleus of 293T cells (Figure 10A). Calculated transfection efficiencies of viable cells were between 50 and 70% for the novel catiomers, 20–30% for mPEG-PLL$_{40}$-, and ~80% for PEI-based polyplexes

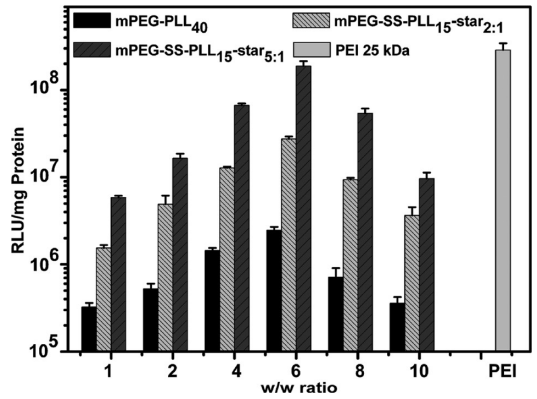

Figure 9. Transfection efficiency of mPEG-SS-PLL$_{15}$-star/pGL-3 polyplexes. 293T cells were incubated for 4 h with mPEG-PLL$_{40}$/pGL-3, mPEG-SS-PLL$_{15}$-star$_{2:1}$/pGL-3, or mPEG-SS-PLL$_{15}$-star$_{5:1}$/pGL-3 complexes fabricated at different weight ratio ranging from 1:1 to 10:1. PEI/pGL-3 (1.3:1, w/w) was used as control. The luciferase activities of these polyplexes were identified 44 h after transfection by luciferase assay and normalized to viable control cells. Data are shown as mean ± SD (n = 5).

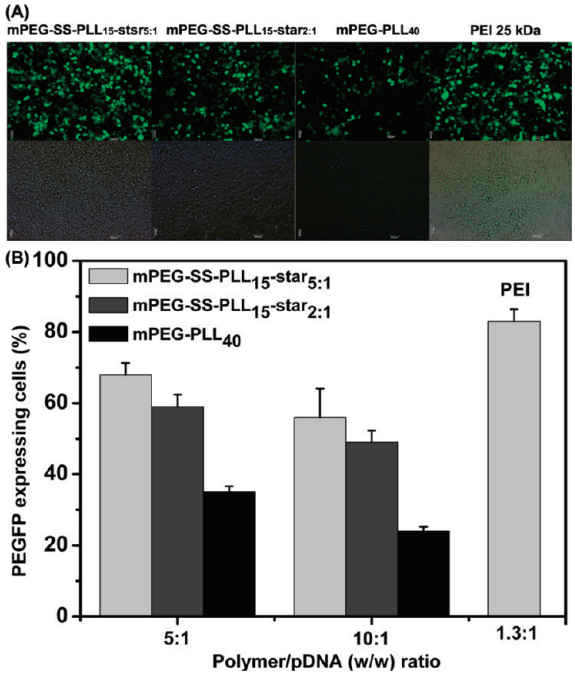

Figure 10. Transfection efficiency of mPEG-SS-PLL$_{15}$-star/pEGFP polyplexes. 293T cells were incubated for 4 h with mPEG-PLL$_{40}$/pEGFP, mPEG-SS-PLL$_{15}$-star$_{2:1}$/pEGFP, or mPEG-SS-PLL$_{15}$-star$_{5:1}$/pEGFP complexes fabricated at 5:1 and 10:1 weight ratio. PEI/pEGFP was used as control. pEGFP-positive cells were identified 44 h after transfection by fluorescence microscopy. Representative images are shown in panel A (5:1, w/w). In addition, viable pEGFP-positive cells were quantified using flow cytometry and normalized to viable control cells (B). Data are shown as mean ± SD (n = 3).

(Figure 10B). Comparison of biological efficacy of polyplexes prepared with 8 kDa mPEG-SS-PLL$_{15}$-star$_{2:1}$ and 12 kDa mPEG-SS-PLL$_{15}$-star$_{5:1}$ did not reveal a significant impact on transfection efficiency. However, the slightly decreased transfection efficiency observed with increasing catiomer concentration (i.e., 10:1 (w/w) vs 5:1 (w/w) implies that excess cationic polymer limits pDNA release from the polyplexes possibly as a consequence of increased stability of these

dx.doi.org/10.1021/bm2017355 | Biomacromolecules 2012, 13, 1024–1034

association complexes.[45] Furthermore, a higher zeta potential could also decrease the gene transfer ability due to increased cytotoxicity or activation of some unknown deleterious cellular response.

3.9. Observation of Intracellular DNA Transport. To visualize the intracellular DNA transport aided by the catiomer, we intercalated pEGFP pDNA with Cy3 to produce fluorescently labeled pDNA that can emit red fluorescence under excitation, thus making it traceable under biological conditions. Before the observation by confocal laser scanning microscopy, 293T cells were first incubated for 4 h with mPEG-SS-PLL$_{15}$-star and PEI-based complexes fabricated at each optimal catiomer/pDNA ratios, and the cell nuclei were stained with DAPI. Confocal images demonstrate that Cy3-labeled pDNA signals (Figure 11, panel 1) could be detected in almost

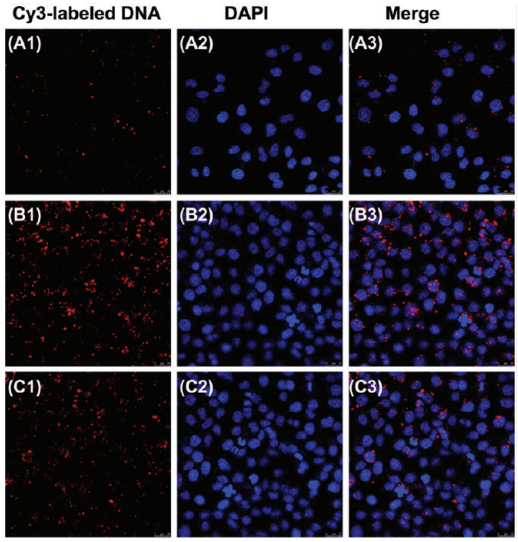

Figure 11. Confocal microscopy images of intracellular trafficking of mPEG-SS-PLL$_{15}$-star/pEGFP polyplexes. 293T cells were incubated for 4 h with mPEG-SS-PLL$_{15}$-star$_{2:1}$/pDNA (A) or mPEG-SS-PLL$_{15}$-star$_{5:1}$/pDNA complexes (B) fabricated at a weight ratio of 5:1. PEI/pEGFP (1.3:1, w/w) (C) was used as control.

all of the cells after 4 h of treatment. More specifically, most of the nuclear fluorescent signal was mainly localized in the perinuclear area in contrast with the DAPI signal in the nucleus (Figure 11, panel 3), whereas some of Cy3-labeled pDNA signal was observed inside the nucleus of 293T cells for mPEG-SS-PLL$_{15}$-star$_{5:1}$/pDNA complexes (Figure 11, panel B3), which clearly reveals that mPEG-SS-PLL$_{15}$-star-based polyplexes could successfully delivery the pDNA into the nucleus.

4. CONCLUSIONS

This study demonstrates successful synthesis of the novel, stimulus-responsive mPEG-SS-PLL$_{15}$-star catiomer. This unique copolymer exhibits high DNA binding affinity, allowing the formation of stable DNA association complexes with an average particle size around 200 nm and tailored surface charges between −20 and +30 mV. As compared with PEI, mPEG-SS-PLL$_{15}$-star shows a superior cellular viability profile and reduced buffering capacity. mPEG-SS-PLL$_{15}$-star polyplexes undergo rapid destabilization in the presence of 10 mM GSH, which mimics redox conditions generally present in intracellular compartments and the extracellular tumor microenvironment. In addition, DNA release was measured from mPEG-SS-PLL$_{15}$-star polyplexes following exposure to pH 5.0 modeling endosomal escape. Finally, biological transfection efficiency using luciferase and GFP demonstrated comparable results, as obtained with bPEI-25k. Considering effective DNA binding ability, minimal cytotoxicity, dual stimulus-responsive degradation mechanisms, and high gene transfection efficiency, the mPEG-SS-PLL$_{15}$-star catiomers appear to offer advantageous properties that support further evaluation as future gene delivery vectors for therapeutic interventions.

AUTHOR INFORMATION

Corresponding Author

*Tel: +86-21-65983706. Fax: +86-21-65983706. E-mail: yongyong_li@tongji.edu.cn, shid@ucmail.uc.edu.

Author Contributions

#Both authors contributed equally to this work.

Notes

The authors declare no competing financial interest.

ACKNOWLEDGMENTS

This work was financially supported by National Natural Science Foundation of China (21004045, 51073121, and 51173136), Shanghai Natural Science Foundation (10ZR1432100), and China Postdoctor Special Fund (201104268).

REFERENCES

(1) Liu, Z. H.; Zhang, Z. Y.; Zhou, C. R; Jiao, Y. P. *Prog. Polym. Sci.* **2010**, *35*, 1144−1162.
(2) Park, T. G.; Jeong, J. H.; Kim, S. W. *Adv. Drug Delivery Rev.* **2006**, *58*, 267−286.
(3) Dong, X.; Tian, H. Y.; Chen, L.; Chen, J.; Chen, X. S. *J. Controlled Release* **2011**, *152*, 135−142.
(4) Itaka, K.; Ishii, T.; Hasegawa, Y.; Kataoka, K. *Biomaterials* **2010**, *31*, 3707−3714.
(5) Dai, F. Y.; Liu, W. G. *Biomaterials* **2011**, *32*, 628−638.
(6) Laporte, L. D.; Cruz, R. J.; Shea, L. D. *Biomaterials* **2006**, *27*, 947−954.
(7) Park, I. K.; Singha, K.; Arote, R. B.; Choi, Y. J.; Kim, W. J.; Cho, C. S. *Macromol. Rapid Commun.* **2010**, *31*, 1122−1133.
(8) Wiethoff, C. M.; Middaugh, C. R. *J. Pharm. Sci.* **2003**, *92*, 203−217.
(9) Varkouhi, A. K.; Scholte, M.; Storm, G.; Haisma, H. J. *J. Controlled Release* **2011**, *151*, 220−228.
(10) Sharma, R.; Lee, J. S.; Bettencourt, R. C.; Xiao, C.; Konieczny, S. F.; Won, Y. Y. *Biomacromolecules* **2008**, *9*, 3294−3307.
(11) Bonamassa, B.; Liu, D. *Adv. Drug Delivery Rev.* **2010**, *62*, 1250−1256.
(12) Pouton, C. W.; Seymour, L. W. *Adv. Drug Delivery Rev.* **2001**, *46*, 187−203.
(13) Riehemann, K.; Schneider, S. W.; Luger, T. A.; Godin, B.; Ferrari, M.; Fuchs, H. *Angew. Chem., Int. Ed.* **2009**, *48*, 872−897.
(14) Itaka, K.; Yamauchi, K.; Harada, A.; Nakamura, K.; Kawaguchi, H.; Kataoka, K. *Biomaterials* **2003**, *24*, 4495−4506.
(15) Nie, Y.; Gunther, M.; Gu, Z. W.; Wagner, E. *Biomaterials* **2011**, *32*, 858−869.
(16) Nomoto, T.; Matsumoto, Y.; Miyata, K.; Oba, M.; Fukushima, S.; Nishiyama, N.; Yamasoba, T.; Kataoka, K. *J. Controlled Release* **2011**, *151*, 104−109.
(17) Erbacher, P.; Bettinger, T.; Belguise-Valladier, P.; Zou, S. M.; Coll, J. L.; Behr, J. P.; Behr, J. L.; Remy, J. S. *J. Gene Med.* **1999**, *1*, 210−222.
(18) Nie, S. M. *Nanomedicine* **2010**, *5*, 523−528.
(19) Han, M.; Bae, Y.; Nishiyama, N.; Miyata, K.; Oba, M.; Kataoka, K. *J. Controlled Release* **2007**, *121*, 38−48.

(20) Hatakeyama, H.; Akita, H.; Ito, E.; Hayashi, Y.; Oishi, M.; Nagasaki, Y.; Danev, R.; Nagayama, K.; Kaji, N.; Kikuchi, H.; Baba, Y.; Harashima, H. *Biomaterials* **2011**, *32*, 4306−4316.
(21) Sakurai, Y.; Hatakeyama, H.; Sato, Y.; Akita, H.; Takayama, K.; Kobayashi, S.; Futaki, S.; Harashima, H. *Biomaterials* **2011**, *32*, 5733−5742.
(22) Hatakeyama, H.; Akita, H.; Harashima, H. *Adv. Drug Delivery Rev.* **2011**, *63*, 152−160.
(23) Knorr, V.; Allmendinger, L.; Walker, G. F.; Paintner, F. F.; Wagner, E. *Bioconjugate Chem.* **2007**, *18*, 1218−1225.
(24) Lai, T. C.; Bae, Y.; Yoshida, T.; Kataoka, K.; Kwon, G. S. *Pharm. Res.* **2010**, *27*, 2260−2273.
(25) Shi, G. F.; Guo, W. J.; Stephenson, S. M.; Lee, R. J. *J. Controlled Release* **2002**, *80*, 309−319.
(26) Simard, P.; Leroux, J. C. *Mol. Pharmaceutics* **2010**, *7*, 1098−1107.
(27) Oumzil, K.; Khiati, S.; Grinstaff, M. W.; Barthélémy, P. *J. Controlled Release* **2011**, *151*, 123−130.
(28) Meng, F. H.; Hennink, W. E.; Zhong, Z. Y. *Biomaterials* **2009**, *30*, 2180−2198.
(29) Sun, H. L.; Guo, B. N.; Cheng, R.; Meng, F. H.; Liu, H. Y.; Zhong, Z. Y. *Biomaterials* **2009**, *30*, 6358−6366.
(30) Takae, S.; Miyata, K.; Oba, M.; Ishii, T.; Nishiyama, N.; Itaka, K.; Yamasaki, Y.; Koyama, H.; Kataoka, K. *J. Am. Chem. Soc.* **2008**, *130*, 6001−6009.
(31) Cai, X. J.; Dong, H. Q.; Xia, W. J.; Wen, H. Y.; Li, X. Q.; Yu, J. H.; Li, Y. Y.; Shi, D. L. *J. Mater. Chem.* **2011**, *21*, 14639−14645.
(32) Kim, Y. H.; Park, J. H.; Lee, M.; Kim, Y. H.; Park, T. G.; Kim, S. W. *J. Controlled Release* **2005**, *103*, 209−219.
(33) Dai, J.; Zou, S. Y.; Pei, Y. Y.; Cheng, D.; Ai, H.; Shuai., X. T. *Biomaterials* **2011**, *32*, 1694−1705.
(34) Sanjoh, M.; Hiki, S.; Lee, Y.; Oba, M.; Miyata, K.; Ishii, T.; Kataoka, K. *Macromol. Rapid Commun.* **2010**, *31*, 1181−1186.
(35) Oba, M.; Miyata, K.; Osada, K.; Christie, R. J.; Sanjoh, M.; Li, W. D.; Fukushima, S.; Ishii, T.; Kano, M. R.; Nishiyama, N.; Koyama, H.; Kataoka, K. *Biomaterials* **2011**, *32*, 652−663.
(36) Pittella, F.; Zhang, M. Z.; Lee, Y.; Kim, H. J.; Tockary, T.; Osada, K.; Ishii, T.; Miyata, K.; Nishiyama, N.; Kataoka, K. *Biomaterials* **2011**, *32*, 3106−3114.
(37) Midoux, P.; Monsigny, M. *Bioconjugate Chem.* **1999**, *10*, 406−411.
(38) Benns, J. M.; Choi, J. S.; Mahato, R. I.; Park, J. S.; Kim, S. W. *Bioconjugate Chem.* **2000**, *11*, 637−645.
(39) Knorr, V.; Russ, V.; Allmendinger, L.; Ogris, M.; Wagner, E. *Bioconjugate Chem.* **2008**, *19*, 1625−1634.
(40) Tang, R. P.; Ji, W. H.; Panus, D.; Palumbo, R. N.; Wang, C. *J. Controlled Release* **2011**, *151*, 18−27.
(41) Georgiou, T. K.; Vamvakaki, M.; Patrickios, C. S.; Yamasaki., E. N.; Phylactou., L. A. *Biomacromolecules* **2004**, *5*, 2221−2229.
(42) Fichter, K. M.; Zhang, L.; Kiick, K. L.; Peineke, T. M. *Bioconjugate Chem.* **2008**, *19*, 76−88.
(43) Cho, H. Y.; Gao, H. F.; Srinicasan, A.; Hong, J.; Bencherif, S. A.; Siegwant, D. J.; Paik, H. J.; Hollinger, J. O.; Matyjaszewski, K. *Biomacromolecules* **2010**, *11*, 2199−2203.
(44) Cheng, H.; Li, Y. Y.; Zeng, X.; Sun, Y. X.; Zhang, X. Z.; Zhuo, R. X. *Biomaterials* **2009**, *30*, 1246−1253.
(45) Lu, B.; Xu, X. D.; Zhang, X. Z.; Cheng, S. X.; Zhuo, R. X. *Biomacromolecules* **2008**, *9*, 2594−2600.
(46) Sheng, R. L.; Luo, T.; Zhu, Y. D.; Li, H.; Sun, J. J.; Chen, S. D.; Sun, W. Y.; Cao, A. *Biomaterials* **2011**, *32*, 3507−3519.
(47) Sonawane, N. D.; Szoka, F. C. Jr.; Verkman, A. S. *J. Biol. Chem.* **2003**, *278*, 44826−44821.
(48) Pack, D. W.; Putnam, D.; Langer, R. *Biotechnol. Bioeng.* **2000**, *67*, 217−223.
(49) Moreira, C.; Olivera, H.; Pires, L. R.; Simoes, S.; Barbosa, M. A.; Pego, A. P. *Acta Biomater.* **2009**, *5*, 267−272.
(50) Fischer, D.; Bieber, T.; Li, Y.; Elsasser, H.; Kissel, T. *Pharm. Res.* **1999**, *16*, 1273−1279.
(51) Liu, Y. M.; Reineke, T. M. *J. Am. Chem. Soc.* **2005**, *127*, 3004−3015.
(52) Kim, T.-I.; Kim, S. W. *React. Funct. Polym.* **2011**, *71*, 344−349.
(53) Christensen, L. V.; Chang, C. W.; Kim, W. J.; Kim, S. W.; Zhong, Z. Y.; Lic, C.; Engbersen, J. F.; Feijen, J. *Bioconjugate Chem.* **2006**, *17*, 1233−1240.
(54) MacEwan, S. R.; Callahan, D. J.; Chilkoti, A. *Nanomedicine* **2010**, *5*, 793−806.
(55) Maeda, T.; Fujimoto, K. *Colloids Surf., B* **2006**, *49*, 15−21.